

Burning Velocity Measurements in Spherical and Cylindrical Vessels

Faranak Rahim, Matthew Ulinski and Hameed Metghalchi

Mechanical, Industrial and Manufacturing Engineering

Northeastern University, Boston, Massachusetts, USA

Metghal@coe.neu.edu

Abstract

Experimental facilities have been built to measure burning velocity of fuel-oxidizer-diluent mixtures. It includes a spherical and a cylindrical vessel. These vessels are equipped with central ignition and several ionization probes to detect flame arrival time at the walls. Spherical vessel is used to measure the pressure rise in a combustion process. A model based on conservation of mass and energy has been developed to determine burning velocity of fuel-oxidizer diluent mixtures. In this model the gas within the vessel is composed of three different regions. The burned gas in the center, the core unburned gas surrounding the burned gas and unburned gas within the thermal boundary layer at the wall. The burned gas includes several shells. Temperature of the burned gases are different in each shell. Burned gases are in chemical equilibrium within each shell. The cylindrical vessel has two large windows for optical measurement. High speed schlieren photography is used to visualize the propagating flame in the cylindrical vessel. Burning velocity of methane-air-diluent and methane-oxygen-argon has been measured over a wide range of temperature, pressure, equivalence ratios and diluent concentration.

Introduction

The laminar burning velocity is a basic physico-chemical property of premixed combustible gases. It directly determines the rate of energy released during combustion in quiescent gas mixtures and is a key parameter in many current models of turbulent combustion [1,2], wall quenching [3]. Therefore a knowledge of the laminar burning velocity is important both for improving our understanding of fundamental combustion processes such as determining reaction mechanism, and for direct practical applications aimed at increasing the fuel efficiency and reducing pollutant emissions.

In addition, current research on developing lean-burning spark ignition engines has shown that a better understanding of the laminar flames velocities is needed to meet Corporate Average Fuel Economy (CAFE) requirements and global warming initiatives (1997 Kyoto Conference on Global Warming).

Finally, the increased use of alternative fuels such as hydrogen, methane, methanol and ethanol will require an improved knowledge of the laminar burning velocities of these fuels.

Although the laminar burning velocity can be determined through the use of basic chemical kinetic models [4,5,6], such models need to be validated and are limited to simple fuels. In contrast, the experimental measurement of laminar burning velocity is relatively simple and accurate. A number of different methods have been used to determine laminar burning velocities. They can be characterized as being either constant pressure [7-22] or constant volume [23-40] methods. The constant pressure experiments, such as those made using flat flame burners [15-17] are limited to a relatively narrow range of temperatures and are most useful for obtaining data at atmospheric pressure. They have the further disadvantages that they provide data at only a

single condition in each experiment and require significant corrections for conductive heat loss to the burner. The constant volume methods, such as combustion in a spherical vessel [34-36], cover a much wider range of temperatures and pressures, provide a range of data along an isentrope in a single experimental run, and require very little correction for heat loss or other effects. The spherical combustion vessel method has been used by many researchers for the determination of laminar burning velocities for a relatively wide range of fuels, diluent concentrations, pressures and temperatures.

Measurements can be made using a spherical vessel and also a cylindrical vessel with glass end windows. Both vessels have been equipped with transducers for making dynamic pressure measurements and ionization probes for measuring arrival times of the flame front at the walls. In addition, optical studies of the flame shape and surface structure will be made in the cylindrical vessel using high-speed cameras. This study will contribute to a better understanding of the physical, chemical, thermodynamic, and fluid mechanical mechanisms involved in combustion over a wide range of conditions and provide data for direct practical applications in the design and testing of numerous combustion devices.

Experimental Apparatus

The spherical combustion vessel is constructed from two hemispheres that are bolted together with a 15.24 cm (6 inch) diameter, shown in Figure 1. The vessel is made from 4140 alloy steel, which can withstand up to 425 atm of pressure. The vessel is fitted with two center ignition electrodes, two ionization probes, a thermocouple, a pressure transducer, and a port for vacuuming and charging.

The cylindrical vessel is shown in Fig. 2. It has an inner diameter of 13.34 cm (5.25 inches) and a length of 13.34 cm (5.25 inches). The body is made of 304 stainless steel and the end windows are 2.54 cm (1.0 inch) thick boronsilicate glass. It is designed to operate over the same pressure and temperature range as the spherical vessel and is equipped with similar access ports. The primary purpose of this facility is to permit optical observation of the flame shape and structure under conditions as close as possible to those in the spherical vessel.

A capacitor discharge ignition system has been used. The two ionization probes are located at the top and the bottom of the each vessel and determine the arrival time of the flame front. They provide information regarding the buoyancy effects

on flame propagation. A K-type thermocouple is used to measure the initial temperature of the fuel mixtures. A Kistler 603B1 piezo electric quartz pressure transducer is used with a Kistler 5010B charge amplifier to measure the dynamic pressure in the vessel.

The charging apparatus consists of a fuel/air/diluent and vacuum system. The fuel/air/diluent mixture concentration has been determined by introducing the gases with right partial pressures. Partial pressures are measured using Kulite silicon on silicon strain gauge transducers. Transducer in the ranges of 0-35, 0-175, and 0-1750 kPa (5, 25, 250 psia) were used. All the gases used are ultra high purity quality (99.99% pure). A vacuum pump capable of maintaining a vacuum of 100 mtorr in the combustion vessel is used.

The data acquisition system consists of a Data Translations 16-bit data acquisition card, which records the pressure change of the combustion vessel at a rate of 10kHz. The analog to digital converter (AD) card receives the pressure signal from the charge amplifier and the signals from the ionization probes. All signals are recorded by a personal computer and an output data file is automatically generated. The computer records pressure-time data up to the maximum pressure. An oscilloscope is also used to monitor the signals of the ionization probes, the pressure transducer and the ignition signal to insure that all the sensors are working and that the system has fired properly.

The experimental procedure consists of vacuuming the combustion vessel to a pressure of 100 mtorr. Once good vacuum has been achieved, the proper mixture of fuel/air is introduced, starting with the gas with the lowest partial pressure. After charging the gases, the vessel is closed and the pipes are vacuumed down and the next gas is introduced into the vessel. The gas mixture in the vessel is allowed to reach equilibrium by waiting several minutes before igniting the mixture. Upon ignition in the spherical vessel, a data file is written to the computer and the pressure signal and ionization probes signals are captured by the oscilloscope. In the cylindrical vessel, the centrally ignited flames are visualized by high speed schlieren photography. The high speed camera that has been used is a Motion Scope PCI Model-9400-0010 and up to 8000 pictures can be taken per second. The flame shape and surface structure can be studied in this vessel using the motion picture.

Gas Motion

Gas particles are started to burn from the center of the vessel where the ignition starts. As the flame propagates, the burned particles will be pushed back to the center and the unburned particles will be compressed and moved away from the flame front. If the volume of the unburned gas is V_{ui} initially, after the flame starts will be V_u and the following equations are true:

$$\frac{V_u}{V_{ui}} = \frac{R^3 - r_u^3}{R^3 - r_{ui}^3} = \left(\frac{P_i}{P}\right)^{\frac{1}{\gamma_u}} \quad (1)$$

$$\frac{r_u}{R} = 1 - \left(\left(\frac{P_i}{P} \right)^{\frac{1}{\gamma_u}} \times \left(1 - \left(\frac{r_{ui}}{R} \right)^3 \right) \right) \quad (2)$$

r_u = Distance of the unburned gas particle from center at time t.

r_{ui} = Initial distance of the unburned gas particle.

R = Radius of the spherical vessel.

P = Pressure at time t.

P_i = Initial pressure in the vessel.

γ_u = Unburned gas specific heat ratio.

Equation 2 can be used to find the unburned gas particle trajectory. After the flame reaches the unburned gas particle, the particle will be burned and then it will be pushed back toward the center and asymptotically reaches to its original place. The burned gas trajectories can be calculated assuming isentropic compression as following:

$$r_b = r_f \times \left(\frac{P_b}{P} \right)^{\frac{1}{3\gamma_b}} \quad (3)$$

r_f = Flame radius at time t, which can be found from experiment.

r_b = Distance of the burned gas particle from center at time t.

γ_b = Burned gas specific heat ratio.

Figure 4 is t-r diagram showing the gas particles and flames front trajectories calculated for the case of stoichiometric methane-air mixture initially at atmospheric pressure and room temperature. This figure again shows that unburned gas particles originally near the center of the bomb have been accelerated to a high velocity and then they are overtaken by the flame front. After the same particles burned at the flame front, they have been pushed back as a result of burned gas compression.

Computational Model

The theoretical model which has been used to calculate flame speed from the pressure rise in a constant volume vessel is based on one previously developed by Metghalchi and Keck [35,36] with some modifications. In this model, gases in the vessel are divided into three parts. The first is the burned gas in the center of vessel, the second is the core unburned gas, which is consumed as the burned gas expands and the third is the gases inside the wall boundary layer.

It is assumed that:

- (1) The flame thickness is negligible for a flame radius greater than two or three centimeters.
- (2) The flame front is smooth and spherical. This assumption can be verified by visualizing the flame in the cylindrical vessel.
- (3) The burned and unburned gases are ideal
- (4) The core unburned gas in the vessel is compressed isentropically from its initial condition during the combustion process.
- (5) The burned gases are divided into shells in which the temperature is uniform but varies from shell to shell. The gases in each shell are assumed to be in chemical equilibrium and isentropically compressed as the pressure rises.

The laminar burning velocity is determined using the equation:

$$S_u = m v_u \dot{x} / A_f \quad (4)$$

where:

S_u = Laminar burning velocity

m = mass of the gas mixture in the vessel

v_u = Specific volume of the unburned gas

\dot{x} = Rate of mass fraction of the gas burned

A_f = the area of the flame.

The mass of the gas mixture can be determined by direct calculation using the initial condition of the mixture. The unburned gas properties are determined using the measured pressure and JANAF Tables [41]. The properties of

the burned gases are also determined using the JANAF Tables and the STANJAN [42] equilibrium code. These properties are used to determine the mass fraction of gas burned, using the equations

$$\frac{V}{m} + \frac{A \delta}{m} = \int_0^x v_b dx' + \int_x^1 v_u dx' \quad (5)$$

$$\frac{E}{m} - \frac{A}{m} \int_0^\delta Pd \delta' = \int_0^x e_b dx' + \int_x^1 e_u dx' \quad (6)$$

where:

- A = Combustion vessel wall area
- e = Specific internal energy
- E = Total initial energy of gas in the vessel
- δ = Boundary layer displacement thickness
- x = Mass fraction burned
- x' = Integration variable
- v = Specific volume
- V = Combustion vessel volume

The subscripts b and u refer to the burned and unburned gas respectively.

The boundary layer displacement thickness, δ , is defined as:

$$\delta = (1/\rho_\infty) \int_0^\infty (\rho - \rho_\infty) dr \quad (7)$$

where:

- ρ = Density of unburned gas within the boundary layer displacement thickness
- ρ_∞ = Density of that portion of unburned gas that is compressed isentropically.

The boundary layer displacement thickness is calculated from the pressure data using the following equation:

$$\delta(t) = \left(\frac{\mu_i}{\pi \rho_i} \right)^{\frac{1}{2}} \left(\frac{\rho_i}{\rho} \right)^{\frac{1}{\gamma_u}} \times \int_0^t \left[\left(\frac{P'}{P_i} \right) - \left(\frac{P'}{P_i} \right)^{\frac{1}{\gamma_u}} \left(\int_{t'}^t \frac{P''}{P_i} dt'' \right)^{\frac{-1}{2}} \right] \quad (8)$$

where:

- ρ_i = the initial density of the gas mixture
- μ_i = the viscosity of the unburned gas at the initial temperature and pressure
- γ_u = the specific heat ratio of the unburned gas
- p_i = the initial pressure of the gas mixture

p', p'' = instantaneous pressure

t = time

t', t'' = integration variables

The conservation equations are solved for the two unknowns: the burned gas temperature of the outer shell and the mass fraction burned at each time step. The two equations are solved by using the two dimensional Newton-Raphson method. For this method, incorporating temperature gradient shells, the two equations are rewritten as:

$$\frac{V}{m} + \frac{A \delta}{m} = \sum_{i=0}^{n-1} v_{bi} x_i + v_{bn} x_n + \quad (9)$$

$$\left(1 - \sum_{i=0}^{n-1} x_i - x_n \right) v_u$$

$$\frac{E}{m} - \frac{A}{m} \int_0^\delta Pd \delta' = \sum_{i=0}^{n-1} e_{bi} x_i + e_{bn} x_n + \quad (10)$$

$$\left(1 - \sum_{i=0}^{n-1} x_i - x_n \right) e_u$$

Where, x_n , v_{bn} and e_{bn} are the mass fraction, specific volume and specific internal energy of the outermost shell in the burned gas region, and x_i , v_{bi} and e_{bi} , the mass fraction, specific volume and the specific internal energy in the shells of the previously burned gas.

Equations 9 and 10 are solved using the Newton-Raphson method for the properties of the n th or outermost shell, where e_{bn} and v_{bn} are functions of the temperature of the n th shell. The n th shell is last shell that has been burned up to the time step of consideration. In the first time step, $n = 1$, the summations equal 0 and the two equations are solved for x_1 and T_{b1} . In the next time step, $n = 2$, e_{b1} and v_{b1} are reevaluated to account for the compression due to the burning of the outer shell (shell 2) and equations 6 and 7 are solved for x_2 , and T_{b2} . This procedure is followed until the last time step, which is the time of maximum pressure in the bomb.

Mass fraction burned is then calculated as a function of time. The rate of the mass fraction burned, \dot{x} , is determined using the mass fraction data from the solution to equations 9 and 10. It is calculated by fitting a parabola to three consecutive mass fraction points and then differentiating to find the slope of the mid point. Each point is used only once to minimize amplification of any possible errors.

The radius, r_f , is calculated as a function of time from the mass fraction burned calculations and the burned gas properties:

$$V_b = xv_b m = \frac{4}{3} \pi r_f^3 \quad (11)$$

An important consideration in the calculation of the flame speed is the effect of flame curvature and stretch rate. The effect of curvature and stretch are greatest when the flame radius is small and diminishes as the flame radius increases. Bradley [7] and Aung and Faeth [43] have investigated the effect of the stretch on flame velocity. Using these investigators' methods, the flame speed of a plane unstretched flame may be calculated using the equation.

$$S_L = S_u + C\alpha \quad (12)$$

where:

S_L = the unstretched burning velocity

S_u = the stretched burning velocity

C is related to the Markstein length and the values have been taken from Bradley's work [13].

and α is the stretch rate:

$$\alpha = \frac{1}{A_f} \frac{dA_f}{dt} \quad (13)$$

$$\alpha = 2 \frac{\dot{r}_f}{r_f} \quad (14)$$

Calculated stretch rates and flame speed corrections for stoichiometric methane/air mixtures as a function of the normalized radius are shown in Figure 5. As can be seen, corrections for curvature and stretch are negligible for dimensionless radii greater than ~0.5, which is the range in which the pressure technique for measuring burning rates can be used.

Results and Conclusion

Spherical and cylindrical vessels have been built. Laminar burning velocities have been measured in spherical vessel using a thermodynamic model. The optical Schlieren photography is being developed to visualize the flame and investigate the flame structure.

Laminar burning velocities have been measured for methane-air and methane-oxygen-argon mixtures over the range of equivalence ratios, ϕ , from 0.8 to 1.2. The laminar burning velocity can be determined in a temperature range of 300-550 K and pressure range of 1-70 atm for methane-air mixture in a constant volume vessel. Moreover, substitution of argon for the nitrogen in air leads to increase in the

maximum temperature at which measurements can be made from ~550 K to ~650 K. Substituting argon for nitrogen increases flame temperature and consequently the concentration of active particles increases, while thermal conductivity and diffusion coefficients are little affected [44]. The maximum pressure in the vessel will be higher using argon instead of nitrogen because of higher flame temperature. The range of unburned gas temperature will increase in the argon case due to higher maximum pressure and larger specific heat ratio of unburned gas since it is being compressed isentropically.

Figures 6 and 7 show the burning velocities of methane-air and methane-oxygen-argon mixtures as a function of fuel/air equivalence ratio at 1 atm pressure and a temperature of 298 K. The increased burning velocity of methane-oxygen-argon mixtures is due to the higher flame temperature. This results from the lower specific heat of methane-oxygen-argon mixtures, as compared to methane-air mixtures. Laminar burning velocities as a function of pressure along four isentropes are shown in Figures 8 and 9 for stoichiometric mixtures of methane-air and methane-oxygen-argon at initial pressures, $P_i = 1, 2, 5$ and 10 atm. Initial temperature for all cases were 298 K.

Acknowledgement

The authors would like to acknowledge Ford Motor Company for their generous financial support. Particular thanks go to Dr. Thomas Kenney of Ford Motor Company and Professor James Keck of MIT for their encouragement and advice and also to, Mimmo Elia, Cedric Fletcher and Farzan Parsinejad for their data providing and problem solving.

Figures

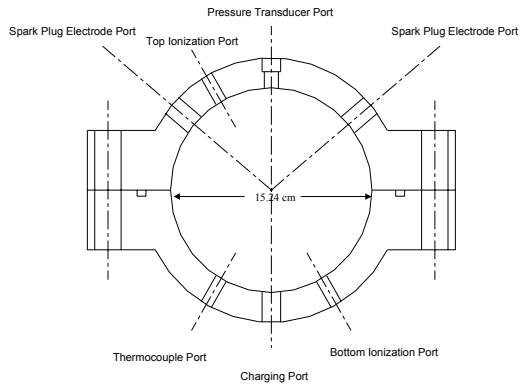


Figure 1: Schematic of spherical vessel.

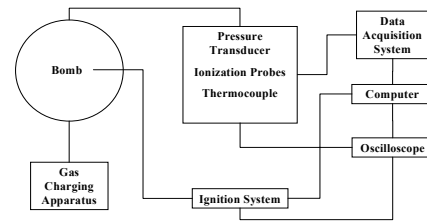


Figure 3: Schematic of the experimental setup.

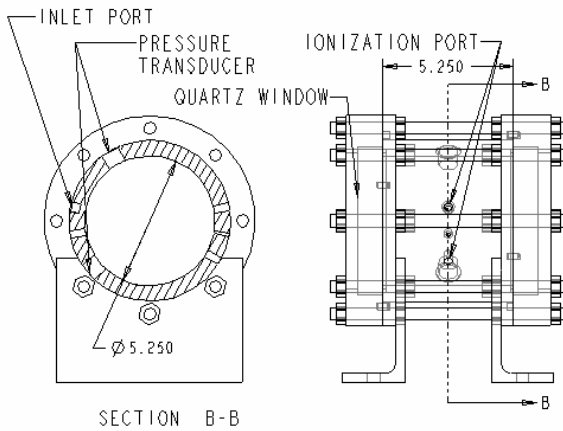


Figure 2: Schematic of the Cylindrical Vessel with Glass End Walls

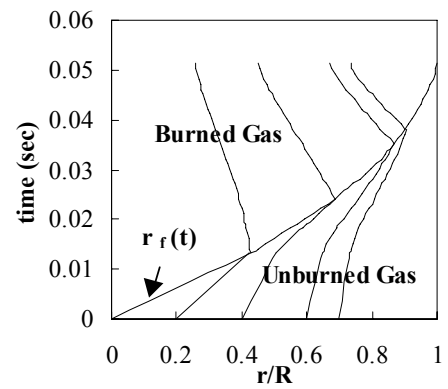


Figure 4: The Gas Particles and Flame Front Trajectories for the Stoichiometric Methane-Air Mixture.

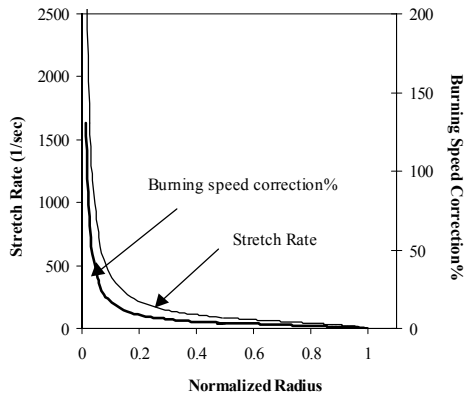


Figure 5. Stretch Rates and Burning Velocity Corrections for Spherical Stoichiometric Methane-Air flame.

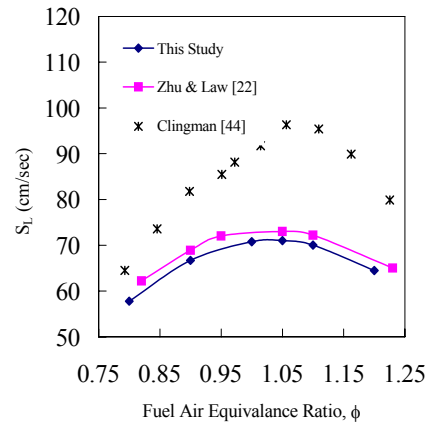


Figure 7 - Laminar Burning Velocity of Methane-Argon-Oxygen Mixture $\phi = 1.0$, $P=1$ atm and $T= 298$ K Compared to Previous Studies.

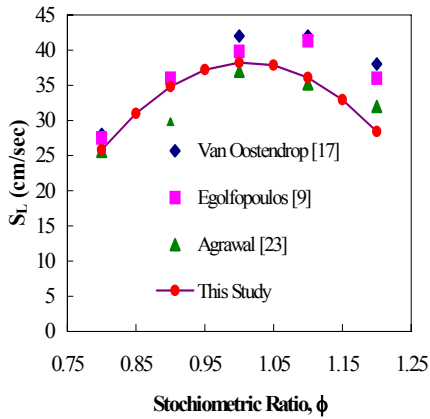


Figure 6 - Laminar Burning Velocity of Methane-Air mixture, $\phi = 1.0$, $P=1$ atm and $T= 298$ K Compared to Previous Studies.

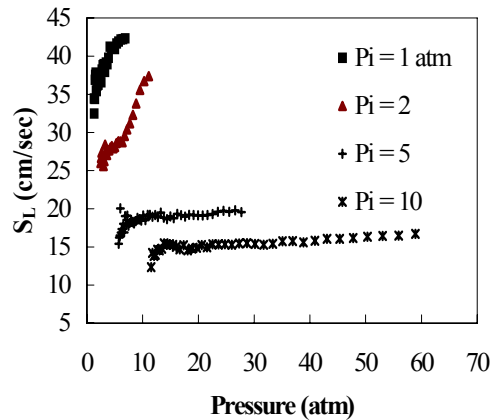


Figure 8- Laminar Burning Velocity vs. Pressure along four isentropes for Methane-Air Mixture, $\phi = 1.0$, $P_i = 1, 2, 5$ and 10 atm and $T_i = 298$ K.

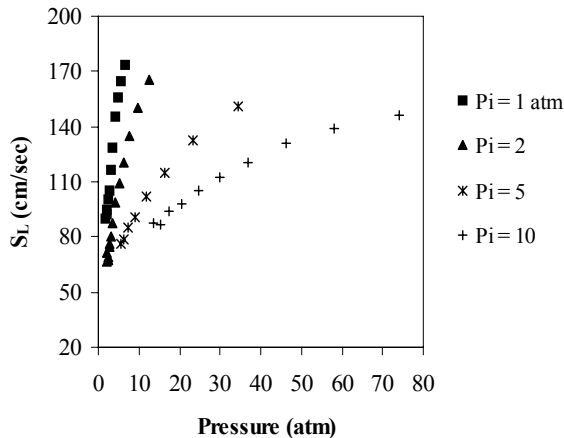


Figure 9 - Laminar Burning Velocity vs. Pressure along four isentropes for Methane-Oxygen-Argon Mixture, $\phi = 1.0$, $P_i = 1, 2, 5$ and 10 atm and $T_i = 298$ K.

References:

[1]. Keck, J.C., Nineteenth International Symposium on Combustion, 1451-1466 (1982).

[2]. Ferguson, C.R. and Keck, J.C., *Combustion and Flame*, 28:197 (1977).

[3]. Frenklach, M., Numerical Approaches to Combustion Modeling, AIAA, Chap. 5 (1991).

[4]. Egolfopoulos, F, Du, D.X. and Law, C. *Combustion Science and Technology* 83:33-75 (1992).

[5]. Corbeels, R. and Scheller, K., Tenth Symposium on Combustion, 66-75 (1965).

[6]. Seshadri, K., Bollig, M. and Peters, N., *Combustion and Flame*, 108:518-536 (1997).

[7]. Bradley, D., Dixon-Lewis, G., and Habik, S. *Combustion and Flame* 77:41-50 (1989).

[8]. Egolfopoulos, F., Du, D. and Law, C. *Combustion Science and Technology* 83:33-75 (1992).

[9]. Egolfopoulos, F.N., Cho, P., and Law, C.K. *Combustion and Flame* 76:375-391 (1989).

[10]. Egolfopoulos, F.N., and Law, C.K. *Combustion and Flame* 80:7-16 (1990).

[11]. Lui, D., and MacFarlane, R. *Combustion and Flame* 49:59-71 (1983).

[12]. Myers, G., and Lefebvre, A. *Combustion and Flame* 66:193-210 (1986).

[13]. Richards, G., Sojka, P., and Lefebvre, A. *Transactions of the ASME: Gas Turbine Conference*, 1988. 111: 84-89 (1989).

[14]. Sher, E., and Ozdor, N. *Combustion and Flame* 89:214-220 (1992).

[15]. Strehlow, R. and Reuss, D. *Progress in Astronautics and Aeronautics*: 61-89 (1980).

[16]. Van Maaren, A., Thung, D. and Goey, L. *Combustion Science and Technology* 96:327-344 (1994).

[17]. Van Oostendrop, D.L. and Levinsky, H.B. *Journal of the Institute Of Energy*. 63:160 -166 (1990).

[18]. Vosen, S. R. *Combustion and Flame*. 82:376- 388 (1990).

[19]. Yamaoka, I., And Tsuji, H. *Twentieth Symposium on Combustion: 1883-1892* (1984).

[20]. Yang, M. and Puri, I. *Combustion and Flame*. 94:25-34 (1993).

[21]. Yu, G., Law, C.K., and Wu, C.K. *Combustion and Flame* 63:339-347 (1986).

[22]. Zhu, D., Egolfopoulos, F, and Law, C. *Twenty-Second Symposium on Combustion: 1537-1545* (1988).

[23]. Agrawal, D. *Combustion and Flame*. 42: 243-52 (1981).

[24]. Chirila, F., Oancea, D., Razus, D. and Ionescu, N. *Revue Roumaine de Chime* 40 (2):101-109 (1995).

[25]. Clarke, A., Stone, R., and Beckwith, P. *Journal of the Institute Of Energy* 68:130-136 (1995).

[26]. Gulder, O. *Combustion and Flame* 56: 261-268 (1984).

[27]. Hamamoto, Y., Izumi, M., and Tomita, E. *JSME International Journal* 33(2): 370-376 (1990).

[28]. Hamamoto, Y., Izumi, M., Tomita, E. and Miyamoto, O. *JSME International Journal* 34(2): 253-257 (1991).

[29]. Hamamoto, Y., Tomita, E., and Izumi, M. *JSME International Journal* 31(1): 140-149 (1988).

[30]. Iijima, T., and Takeno, T. *Combustion And Flame* 65:35-43 (1986).

[31]. Kageyama, T., Fisson, F. and Ludwig, T. *Progress in Astronautics and Aeronautics*. 151: 323-330 (1993).

- [32]. Koroll, G., Kumar, R., and Bowles, W. Emerging Energy Technology -- ASME, Petroleum Division 50:31-40 (1993).
- [33]. Kwon, S., Tseng, L., and Faeth, G. Combustion and Flame 90:230-246 (1992).
- [34]. Metghalchi, Mohamad. Ph.D. Thesis, Massachusetts Institute of Technology. (1980).
- [35]. Metghalchi, Mohamad, and Keck, James C. Combustion and Flame 48: 191-210 (1982).
- [36]. Metghalchi, M., and Keck, J. Combustion and Flame 38:143-154 (1980).
- [37]. Oancea, D., Razus, D. and Ionescu, N. Revue Roumaine de Chime 39(10): 1187-1196 (1994). Rhodes, D. and Keck, J. Proceedings of the SAE: 23-35 (1985).
- [38]. Ryan, T.W., and Lestz, S.S. Proceedings of the SAE: 652-664 (1981).
- [39]. Shebeko, Y., Tsarichenko, A., Trunev, A., Navzenya, V., Papkov, S., And Zaitzev, A. Combustion and Flame 102:427-437 (1995).
- [40]. Tseng, L., Ismail, M., and Faeth, G. Combustion and Flame 95:410-426 (1993).
- [41]. JANAF Thermochemical Tables, Third Edition. American Chemical Institute, American Institute of Physics, National Bureau of Standards (1986).
- [42]. Reynolds, W.C., Stanford University Report, ME 270, no 7. (1986).
- [43]. Aung, K. T., Hassan, M. I., and Faeth, G. M., Combustion and Flame, 109:1, (1997).
- [44]. Clingman, H., Brokaw R. S. and Pease R. N., Fourth Symposium (International) Combustion, (1953).